Actinometry - Use of Particle in Cell code to generate improved rate constants for determination of absolute O density.

J. Conway[1], S. Kechkar[1], N. O' Connor, C Gaman[1], M. M. Turner[1] and S. Daniels[1].

[1]National Centre for Plasma Science and Technology, Dublin City University, Glasnevin, Dublin 9, Ireland.

E-mail: jim.conway@dcu.ie

Abstract
Actinometry is a non-invasive optical technique that can be used to quantitatively monitor atomic oxygen number densities [O] in gas discharges under certain operating conditions. However, careless application of the technique can lead to erroneous conclusions regarding the behaviour of atomic oxygen in plasma. One limitation on this technique is an accurate knowledge of the various rate constants required, which in turn is hampered by an insufficiently precise knowledge of the Electron Energy Distribution Function (EEDF) in the plasma. In this work Particle in Cell (PIC) simulations have been used to generate theoretical EEDFs. To validate a simulation the electron density n_e produced by the PIC code is compared to experimental n_e values measured using a hairpin probe. The PIC input parameters are adjusted to optimise agreement between the PIC and experimental n_e results. This approach should in principle yield an EEDF that more accurately reflects the true EEDF in the plasma. The PIC EEDF is then used to generate rate constants for the actinometry model which should improve the accuracy of the quantitative [O] result for that particular set of plasma conditions. The actinometry [O] results are then compared to [O] results obtained using Two-photon Absorption Laser Induced Fluorescence (TALIF) to validate the approach.

1. Introduction

Oxygen based plasmas containing either pure oxygen, or oxygen gas mixtures find a wide range of application in manufacturing industries such as the semi-conductor manufacturing industry. The array of tasks performed by these plasmas is diverse and depends on the plasma composition which is primarily determined by the choice of feedstock gases as well as the settings chosen for operational parameters such as RF power, gas flow rate and pressure selected during plasma operation. Oxygen is commonly used in processes such as Reactive Ion plasma Etching (RIE) [1], Plasma Enhanced Chemical Vapour Deposition (PECVD) [2], organic polymer etching [3] and oxidation of thin films [4]. Fabrication of structures on the nano-scale typically involves reactive gas mixtures often containing oxygen along with gases such as fluorine, chlorine and hydrogen. Atomic oxygen is critical for side-wall surface passivation enabling anisotropic trench etching via the formation of a dielectric oxide layer inside the microscopic etch trenches on the silicon substrates [5]. While many semiconductor plasmas tend to operate at low to medium pressures, recent development of industrial atmospheric plasma sources has seen high pressure plasmas containing oxygen used for applications such as the treatment of sensitive surfaces in the bio-medical industry [6]. The atomic oxygen radical has been identified as a key species in determining the behaviour of many of these processes and so there is much interest in developing a robust diagnostic capable of accurately monitoring absolute atomic oxygen number density values [O] in processing plasmas under a range of operating conditions.

Much effort has been focussed on the development of non-invasive plasma diagnostics for industrial plasmas to enable monitoring of the plasma composition and conditions within the plasma chamber without disturbing the process. Traditional plasma probes such as Langmuir probes which are used to measure electrical characteristics and charged species densities in plasma [7], or catalytic probes which are used to measure atomic O densities [8, 9] are commonly used in research plasma sources to characterise the plasma. However, these are invasive probes and so are undesirable in a manufacturing

environment as the probe can disturb the plasma and also possibly introduce contaminants into the process chamber which can deposit onto the wafer and impact the operation of the final product in a negative manner. Non invasive techniques such as downstream NO_2 titration can be used to measure atomic oxygen density [10] but this has the obvious disadvantage of making the measurement away from the plasma chamber and so the results may not reflect the true situation in the process chamber as recombination may have a large impact on [O] as it flows from the chamber to the titration apparatus. In-situ diagnostics such as the Two-photon Absorption Laser Induced Fluorescence (TALIF) method is a non-invasive technique that allows quantitative measurement of absolute atomic oxygen number densities [11]. However, this is an expensive technique that is difficult to implement and does not lend itself readily to industrial fabrication environments as industrial standard plasma tools may not have the optical access required to implement such an experiment.

For in-situ measurements of [O] at the process chamber optical emission based techniques offer the best possibility of developing a non-invasive diagnostic. The use of optical emission to monitor [O] in industrial plasma was first performed by Harshbarger *et al* [12]. In this paper an examination of actinometry as a method for monitoring atomic oxygen ground state number density in an industrial RF capacitive etch plasmas is undertaken. Actinometry, which was first proposed by Coburn and Chen to monitor atomic fluorine density in RF capacitive systems [13] is based on measuring the ratio of two optical emission lines from the plasma; one from the species of interest and the other from trace amounts of a noble gas actinometer of known concentration (typically argon at < 5%) which is added to the system to allow implementation of the technique. The actinometer is deliberately introduced at low concentration to avoid disturbing the plasma. By taking the ratio of the two emission lines in the plasma, variations in line intensity caused by changes in the electron density n_e can be compensated for making it simpler to relate the line emission intensity to [O]. This approach is simple to implement, relatively cheap, and most importantly is non-invasive. Thus, actinometry offers a way of monitoring atomic oxygen number density and more importantly flagging variations in [O] as even modest changes can affect the outcome of the etch process and render the final product unsuitable for purpose. Work done by previous authors has shown that application of the actinometry method does not always yield results that reflect the true atomic oxygen number density in the plasma. The validity of actinometry for atomic oxygen has been investigated for various plasma sources: RF capacitive plasma [14, 15, 16], ECR source [17], DC glow discharge [18], microwave source [19, 20], helicon source [21], inductive source [22], and micro-scale atmospheric pressure jet source [23].

Walkrup *et al* [14] investigated the validity of actinometry for atomic oxygen in RF capacitive plasmas containing both pure O_2 and O_2/CF_2 mixtures by examining line emission intensity ratios. The plasma emission for atomic oxygen at 844 nm $O^*(844)$, 777 nm $O^*(777)$ and argon at 750 nm $Ar^*(750)$ were recorded and the $O^*(844)/Ar^*(750)$ and $O^*(777)/Ar^*(750)$ ratios were monitored and compared with [O] results obtained using TALIF at a fixed total pressure of 400 mTorr. The percentage of CF_4 was varied from zero and atomic oxygen density measured for the various gas mixtures. Their findings indicate that the $O^*(844)/Ar^*(750)$ ratio correlated well with [O] changes under these conditions. However, the $O^*(777)/Ar^*(750)$ ratio gave questionable results. This is attributed to the large contribution made by dissociative excitation of O_2 to the generation of the 777 nm oxygen line emission in the plasma while dissociative excitation makes a significantly smaller contribution to 844 nm emission. As a result, the actinometry [O] values obtained using the $O^*(844)/Ar^*(750)$ ratio more accurately reflects the true atomic oxygen density in the system. Their results for pure O_2 plasmas however, did not show good correlation between atomic oxygen densities and the actinometry signals, a result that is borne out by Collert *et al* [15]. Katsch *et al* [16] investigated the validity of the technique in low pressure O_2 RF capacitive plasmas for pressures in the 75 – 600 mTorr range and RF powers varying from 10 – 100 W. They proposed an improved actinometry that incorporates corrections into the standard actinometry model to take account of both the increase in emission for the 777 nm and 844 nm lines of atomic oxygen due to the dissociative excitation contribution and also any reduction in emission caused by quenching of the excited atomic oxygen or argon states, primarily by O_2 for their plasma conditions. Their approach also requires a model based calculation of the EEDF in the plasma which is then used to generate rate constants for use in the actinometry calculations. Comparing their [O] results to measurements made using TALIF they concluded that actinometry was a valid technique for measuring atomic oxygen number density, particularly when using the $O^*(844)/Ar^*(750)$ emission ratio for the range of experimental conditions examined, though some care

had to be exercised in the validity of the EEDF produced by the model under certain conditions where it was found to be unreliable. Booth *et al* [17] examined atomic oxygen actinometry in a low pressure ECR source containing pure O_2 and O_2 gas mixtures containing SF_6, N_2 and Kr. They used the $O^*(844)/Ar^*(750)$ emission ratio and compared it with quantitative measurements of [O] made using Vacuum Ultraviolet (VUV) absorption spectroscopy and concluded that the method is not valid under conditions where the dissociation fraction is lower than 10 %. Their results indicated that under such conditions the actinometry measurements better reflected the O_2 density $[O_2]$ rather than the O density and concluded that dissociative excitation of O_2 molecules was the primary source of 844 nm emission rather than direct excitation of O atoms in the plasma for their range of operating conditions. Pagnon *et al* [18] examined actinometry in DC O_2/Ar glow discharges produced in a Pyrex tube over the 100 – 500 mTorr pressure range with discharge currents of 5 – 80 mA and used VUV absorption spectroscopy to quantitatively measure [O] in the plasma. They concluded that the method was valid under their range of experimental conditions and that the results obtained using the $O^*(844)/Ar^*(750)$ emission ratio was more accurate than those obtained using the $O^*(777)/Ar^*(750)$ emission as the effects of dissociative excitation were smaller for $O^*(844)/Ar^*(750)$ emission than for $O^*(777)/Ar^*(750)$ emission. They also found that inclusion of a correction factor for dissociative excitation at lower pressures and currents where the dissociation fraction was found to be < 1% allowed reasonable quantitative results to be obtained for their system. Granier *et al* [19] applied the method to determine [O] in an O_2/N_2 microwave surface wave discharge. They monitored atomic oxygen emission at 777 nm and 844 nm in the usual manner. However, due to problems with emission from the first positive system of nitrogen they used a slightly different argon emission line for 844 nm actinometry and monitored the $O^*(777)/Ar^*(750)$ and $O^*(844)/Ar^*(811.5)$ emission ratios. The values obtained from actinometry were compared to values measured using VUV absorption spectroscopy and were found to agree reasonably well. Again they found that the method works best for the $O^*(844)/Ar^*(811.5)$ emission ratio particularly if the dissociation fraction was greater than a few per cent. Ershov *et al* [20] investigated atomic oxygen actinometry in an Ar/O_2, 2.45 GHz microwave source and used downstream NO_2 gas titration to measure [O] for comparison. They concluded that actinometry using the $O^*(844)/Ar^*(750)$ emission ratio was valid for modest Ar/O_2 flow ratios (smaller than 2) when the total pressure in their system exceeded 1 Torr while the $O^*(777)/Ar^*(750)$ ratio gave misleading results. Bousquet *et al* [21] used actinometry in a low pressure (5 mTorr) pulsed O_2/Hexamethyldisiloxane helicon source to monitor atomic oxygen density. They determined that direct excitation of atomic oxygen was the main source of emission at 844 nm with only a small contribution due to dissociative excitation of O_2 and that the actinometry technique using the $O^*(844)/Ar^*(750)$ emission ratio was valid under these experimental conditions provided dissociative excitation of O_2 was also taken into account. Taylor *et al* [22] used actinometry in a low pressure (10 mTorr) inductively coupled plasma using the $O^*(844)/Ar^*(750)$ emission ratio to monitor atomic oxygen density as a function of RF power and oxygen partial pressure in O_2/ noble gas mixtures where He, Ar and Xe were alternatively used as the noble gas. They used Appearance Mass Spectrometry (AMS) to independently measure [O] trends in the plasma. They found that actinometry gave results that matched the atomic oxygen measurements obtained using AMS. Neimi [23] *et al* monitored atomic oxygen density in a He/O_2 atmospheric plasma jet using the using the $O^*(844)/Ar^*(750)$ emission ratio actinometry scheme. Special care had to be given to quenching effects of both the O and Ar excited states as quenching rates dominate optical transition rates at these high pressures. The results were compared with [O] values obtained using TALIF and found to give excellent agreement. Various publications cited indicate that dissociative excitation is a major contributor to inaccuracies in the [O] density results obtained using actinometry.

The literature reviewed indicates that when the dissociative excitation contribution is large the actinometry approach yields questionable results for [O] and that oxygen emission from the plasma more likely follows the $[O_2]$ density. A dissociative excitation factor is incorporated in the actinometry model to allow for this [17, 18]. Another source of error is the fact that the absolute number densities derived using actinometry depend on the use of rate constants which are sensitive to the form of the EEDF in the plasma [15, 17]. Assuming the electrons follow a Maxwellian distribution within low pressure capacitive plasma for the purpose of actinometry calculations is too simplistic and previous experimental work has shown that this assumption is not strictly true [24]. However, it is a convenient place to start and some actinometry results presented to date use this distribution [25]. This approach

can lead to inaccuracies in the required rate coefficients, and so the corresponding [O] densities derived using actinometry. Measurement of the EEDF using Langmuir probes is also problematic for capacitive plasma systems contains negative ions such as the oxygen plasmas investigated in this work particularly for the high energy electrons which are the most important for inelastic processes such as ionisation, dissociation and excitation. Consequentially, a modelling approach was adopted to determine an appropriate EEDF for this work. A 1D - PIC plasma simulation was used to generate optimized EEDFs. The validity of the EEDF was checked by comparing the electron density from the simulation to that experimentally measured using a hairpin probe. A good match in the electron densities was assumed to indicate a valid PIC simulation and the corresponding EEDF was used to generate the rate constants used in the actinometry calculations. The PIC simulation was "tuned" to the plasma by varying the PIC input parameters and comparing the electron density produced by the code to experimentally measured values of n_e until reasonable agreement between experiment and simulation is reached. The input for the PIC simulation takes account of the chamber geometry, DC bias at the powered electrode, secondary electron yield coefficients γ_{se}, and other process parameters such as the feedstock gas composition and temperature.
TALIF experiments were performed simultaneously with the actinometry experiments to independently monitor [O] in the plasma. The TALIF technique is known to be reliable and so the results obtained with this method could be compared to those obtained using actinometry to validate the improved actinometry model based on the new approach to generating EEDFs.

2. Experimental Set up

The Chamber used in these experiments is an Oxford Instruments Plasmalab System 100 reactive ion etcher (figure 1) which has been described previously [26].

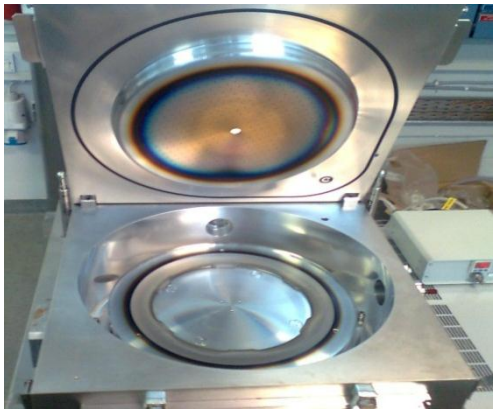

Figure 1: Oxford instruments Plasmalab 100 capacitive RF plasma etch chamber.

This is a parallel plate capacitive asymmetric RF plasma system. The tool is designed to process 200 mm wafers that are placed on the lower powered electrode. Feedstock gas is fed into the chamber via a showerhead which is designed into the upper ground electrode. A gas mixture of 96:4 % O_2:Ar is introduced into the chamber for the experiments performed in this work and plasma struck under various RF power at a pressure of 100 mTorr and the atomic oxygen content determined using TALIF. For the actinometry measurements, optical emission from the plasma was recorded using a Horiba Jobin Yvon Auto MicroHR spectrometer which contains two 32 mm x 32 mm diffraction gratings each with 1200 grooves/mm. One grating is blazed at 330 nm while the other is blazed at 630 nm. The spectrometer was calibrated using a Heraeus Tungsten halogen lamp LSB 020 which was installed on lamp mount LSA 367 connected to a LSL 111 stabilised power supply to get the spectral response function for the instrument. Special attention was paid to the relative correction factors between the 884 nm, 777 nm and 750 nm lines. The atomic oxygen lines at 777 nm and 844 nm and the argon line at 750 nm were recorded for each of the plasma operating conditions to enable determination of the absolute number density for oxygen in the plasma.

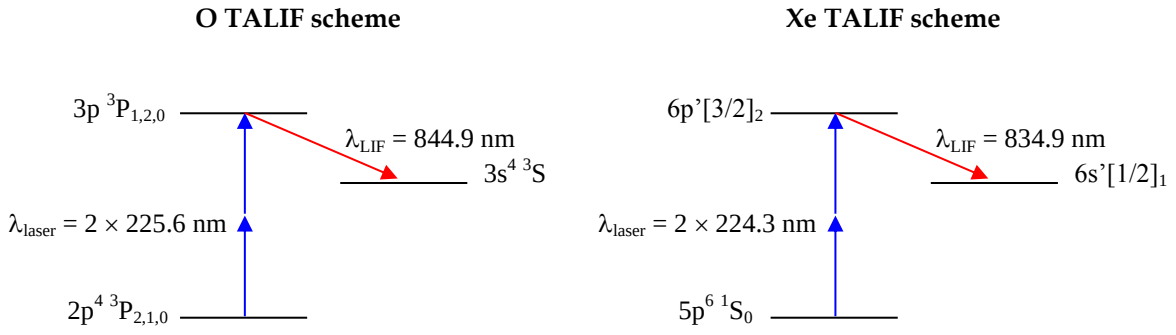

Figure 2: TALIF schemes for atomic oxygen and xenon used in this work.

The 2 photon LIF scheme used is one proposed by Döbele *et al* [11]. A diagram of the atomic transitions involved is given in figure 2 above. A 2-photon excitation at 225.6 nm, and the subsequent LIF at 844.9 nm are used to investigate the atomic O densities in the plasma. To calibrate the system for absolute atomic oxygen number density determination Xe gas was introduced into the chamber at a fixed pressure and a 2 photon excitation of Xe gas at 224.3 nm and the subsequent LIF at 834.9 nm were recorded. For TALIF experiments an Innolas Spitlight 600 Nd:YAG laser is used to pump a Radiant Dyes Narrowscan dye laser. The laser system output has a bandwidth of < 0.03 cm^{-1} and is operated at a frequency of 10 Hz. The second harmonic of the Nd:YAG laser at 532 nm was fed into a dye mixture of DCM/Pyridine 1 in methanol. The dye mixture was found to produce a useful lasing wavelength range of 640 nm to 705 nm. The light from the fundamental of the dye laser is passed through frequency doubling and tripling crystals and finally through a Pellin Broca system of prisms to separate out the UV radiation from the dye fundamental and doubled wavelengths.
A diagram of the experimental set-up used in this work is shown in figure 3 below. The exit UV radiation from the laser was steered to the process chamber using UV extended aluminium mirrors. A UV grade fused silica plano-convex lens of focal length 100 cm was used to focus the laser beam at the centre of the chamber via a UV extended fused silica viewport. The back reflection from the lens was steered onto a Thorlabs Det210 fast photodiode and used to trigger the oscilloscope.

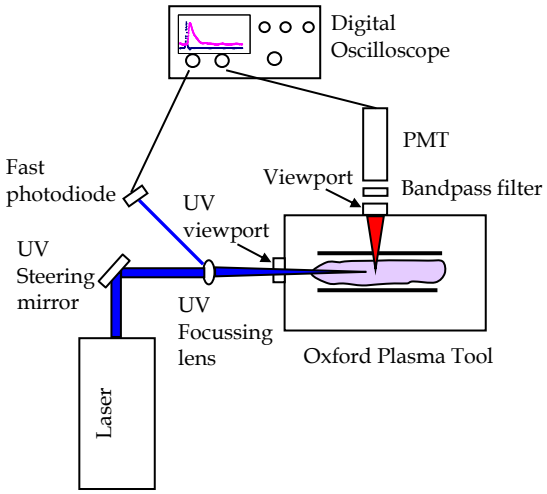

Figure 3: Schematic of TALIF experimental arrangement used in this experiment. The spectrometer (not shown in the diagram) recorded emission from the plasma through a viewport at the front of the chamber.

The resulting fluorescence was recorded at 90^o to the laser propagation direction using a Hamamatsu R632-01 photomultiplier tube. A LOT-Oriel optical bandpass filter centred at 850 nm with a 40 nm

bandwidth is placed at the entrance to the PM tube to attenuate all other light emitted from the plasma except the fluorescent light. The signal from the PM tube was recorded on a Tektronix DPO 3034 300 MHz digital oscilloscope.
Absolute atomic oxygen number density was determined from TALIF experiments using the expression:

$$[\mathrm{O}] = \chi \frac{\mathrm{S_O}}{\mathrm{S_{Xe}}}[\mathrm{Xe}] \qquad (1)$$

with

$$\chi = \frac{\mathrm{T_{Xe}}}{\mathrm{T_O}} \frac{\eta_{Xe}}{\eta_O} \frac{\sigma_{Xe}^{(2)}}{\sigma_O^{(2)}} \frac{a_{21}^{Xe}}{a_{21}^{O}} \left(\frac{\lambda_{Xe}}{\lambda_O} \right)^2$$

where S_O and S_{Xe} are the measured atomic oxygen and xenon LIF signals integrated over time, fluorescent wavelength, excitation wavelength and normalised to the square of the laser pulse energy. χ is a constant that takes account of the optical component transmission for the system, the quantum efficiency of the detector at the fluorescent wavelength, the two-photon absorption cross section, the effective branching ratio and the wavelength of the fluorescence and [Xe] is the xenon number density used during the calibration process.
Reliable n_e data is required to compare with the n_e values from the PIC to validate the simulations. To this end a hairpin probe was used. The floating hairpin probe technique has been described previously [27]. The hairpin probe is constructed by folding a piece of wire into the shape of a hairpin. If the dimensions are correct the hairpin acts as a microwave resonator. The resonant frequency of the hairpin structure depends on the length L of the pins and the dielectric constant ε of the medium in which the hairpin is immersed, and is given by:

$$f_r = \frac{c}{4L\sqrt{\varepsilon}} \qquad (2)$$

where c is the speed of light. In vacuum $\varepsilon = 1$ and the vacuum resonance frequency f_o is c/4L. For weakly magnetized plasma, the dielectric constant is given by:

$$\varepsilon = 1 - \frac{\omega_p^2}{\omega^2} \qquad (3)$$

where ω_p is the electron plasma frequency.

Using the two expressions above the electron density n_e in the plasma can be written as:

$$n_e = \frac{{f_r}^2 - {f_0}^2}{0.81} \ (10^{10}\ \mathrm{cm^{-3}}) \qquad (4)$$

where f_r and f_0 are in GHz.

In these experiments the hairpin probe was driven by a Hewlett Packard HP8350 microwave generator with a sweep range from 1 GHz to 8.0 GHz. The microwave frequency was typically varied between 2.0 – 4.0 GHz and a directional coupler connected between the microwave source output and the 50 Ω coaxial line whose extreme end is terminated by a single turn loop antenna measures the reflected power from the terminated end. The magnitude of the reflected signal which varies with frequency is converted into a negative dc output using a Schottky diode and captured on an oscilloscope (Tektronix TDS3034B 300 MHz). At the resonance frequency, maximum power is coupled into the hairpin

resulting in a sharp drop in the reflected signal. Correspondingly the output signal from the diode drops to almost zero at the resonant frequency allowing f_r , and thus n_e to be obtained precisely.
The chamber temperature for the various operating conditions investigated in this work was recorded using a K type Watlow thermocouple.

3. Results and discussion

The intensity I_O of an emission line such as that at 844 nm resulting from a radiative transition in atomic oxygen is given by the expression:

$$I_O = Ch\nu_{ij}A_{ij}\int_{E_{ij}}^{\infty} v_e(E)\sigma_i(E)f(E)dE\,\frac{n_e[\mathrm{O}]}{\Sigma A_{ij}+k_Q[Q]} \qquad (5)$$

where C is a calibration constant depending on the spectrometer and associated optics, ν_{ij} is the frequency of the emitted light, σ_i(E) is the cross section for excitation of the emitting atomic state, f (E) is the electron energy distribution function within the plasma, A_{ij} is the Einstein coefficient for the transition under consideration and ΣA_{ij} is the sum of all transition from the excited state, n_e is the electron density in the plasma, [O] is the ground state atomic oxygen density in the plasma, k_Q is the quenching coefficient for atomic oxygen by quenching species Q, and [Q] is the number density of the quenching species which is predominantly O_2 for the plasma under consideration in this work. This expression shows that changes in intensity can be attributed to changes in f (E), n_e or [O] within the plasma. By taking the ratio of two emission lines, each one taken from a different species in the plasma (as used in the actinometry technique), intensity variations due to changes in n_e are cancelled out and so any changes in the optical ratio can then be attributed to fluctuations in [O] or in f (E).
In this work an improved actinometry approach that expands on traditional actinometry for atomic oxygen by incorporating both excitation of the upper level via dissociation channels and collisional quenching of excited states is adopted [16]. Using this approach the atomic oxygen density [O] can be determined using the expression:

$$[\mathrm{O}] = \frac{I_O}{I_{Ar}}[\mathrm{Ar}]\frac{k_e^{Ar}}{k_e^{O}}\frac{1}{\gamma} - \frac{k_{de}^{O}}{k_e^{O}}[\mathrm{O_2}] \qquad (6)$$

with

$$\gamma = \frac{\mathrm{C_O}\nu_{\mathrm{O}}A_{ij}^{\mathrm{O}}\left(k_q^{\mathrm{Ar}}[\mathrm{O_2}] + \sum_j A_{ij}^{\mathrm{Ar}}\right)}{\mathrm{C_{Ar}}\nu_{\mathrm{Ar}}A_{ij}^{\mathrm{Ar}}\left(k_q^{\mathrm{O}}[\mathrm{O_2}] + \sum_j A_{ij}^{\mathrm{O}}\right)}$$

where k_e is the rate coefficient for excitation of the upper level via electron collision, I_O and I_{Ar} are the spectral intensities of the oxygen and argon emission lines recorded from the plasma, and γ is a number which incorporates optical and geometric parameters such as solid angle and transmissions as well as quenching term for the excited states and Einstein coefficients for spontaneous emission from the excited state. Thus, the first term of equation (1) is just classical actinometry with quenching included while the second term incorporates excitation of the excited state during the dissociation of O_2 molecules in the plasma. The validity of actinometry is strongly determined by the excitation mechanism for the upper level of the oxygen atom. If ground state excitation of atomic O is the dominant excitation mechanism then actinometry works reasonably well. However, if dissociative excitation is the dominant excitation process then actinometry for atomic O is not reliable and the emission will reflect O_2 number densities rather than atomic O densities in the plasma [17].
While the approach adopted includes dissociative excitation and quenching effects, the quality of the excitation rate coefficients k_e used also plays a key role in the overall accuracy of the technique. The rate constants in turn depend on the EEDF f (E) in the plasma as can be seen from the expression:

$$k_e = \int_0^\infty f(E)\sigma(E)\sqrt{\frac{2E}{m_e}}dE \qquad (7)$$

where $f(E)$ is the normalised EEDF, m_e is the electron mass, $\sigma(E)$ is the electron collisional excitation cross section and E is the electron energy. This implies that attaining reliable rate constants values requires accurate cross section and EEDF data.

In this work the main thesis is that the PIC model is "good" if the n_e value obtained from the simulation output matches the experimental values measured in the plasma. Adopting this approach, the EEDF generated in the PIC simulation when the PIC n_e matches the measured n_e values should in principle give k_e values that yield improved agreement between actinometry and TALIF results for [O] measured on the system. The input parameters into the code were varied until the PIC electron density output agreed with that measured with the hairpin probe.

For each RF power setting the voltage input was recorded off the plasma tool to use as an initial input parameter for the initial PIC simulation. The chamber geometry and gas composition remain unchanged over the course of the experiments. The gas temperature was recorded and noticed to increase with increasing RF power so temperature variations were included in the PIC simulations.

The value of the secondary electron emission coefficient γ_{se} was varied slightly for each power setting. For low energy ion neutralisation at a surface the secondary electron ejection is independent of the positive ion energy and Auger relaxation is the main mechanism for electron ejection from the surface. Kinetic ejection where the ion energy plays a role typically becomes important at energies in the keV range. However it has been found that for oxygenated surfaces, kinetic ejection can become important at significantly lower ion energies as the oxide layer on the surface lowers the work function of the surface. Kinetic ejection can become important at hundreds of eV rather than keV [28, 29]. Increasing the RF power increased the DC bias across the powered sheath resulting in an increase in the kinetic energy of positive ions accelerated from the plasma to the chuck. The recorded values were in the hundreds of V range. This indicates that γ_{se} should increase somewhat as the RF power increases particularly for the higher RF powers.

The results obtained using the original parameters measured from the plasma tool, along with those obtained when the match between the PIC n_e and experimental n_e are optimised are shown in figure 4 below. The corresponding EEDFs from each simulation were then used to calculate the rate coefficients for use with the actinometry model for both cases.

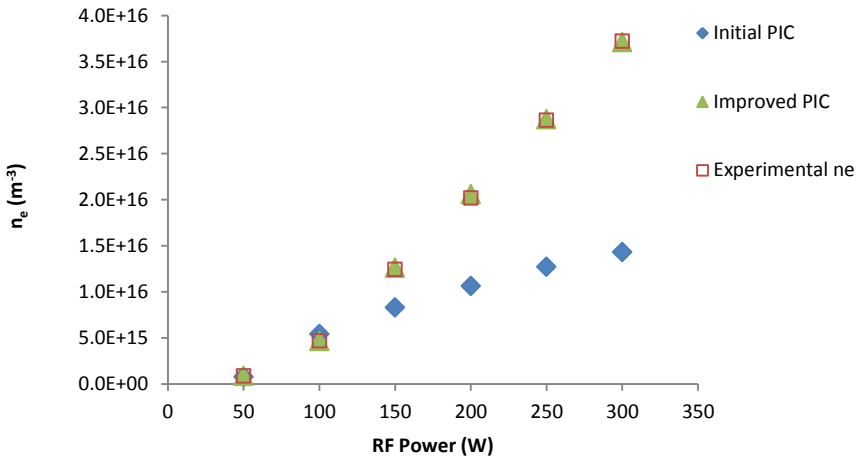

Figure 4: Plot of electron density vs RF power. The experimental data was recorded using a hairpin probe.

The emission spectra recorded were processed before the final data is taken for use in the actinometry expressions to calculate [O]. The spectrum was first smoothed using a 5 point FFT routine with the SynerJY software package and then optimal Gaussian fits to the 750 nm, 777 nm and 844 nm peaks

were obtained. The peak value and area under the peak from the Gaussian fit were then used for actinometry analysis.
Sample line profiles are shown in figure 5 below. Comparing the profiles, the line widths were not comparable which should be the case as all gas species in the plasma chamber should be at the same gas temperature. However, dissociative excitation results in "hot" fragments (i.e. atomic O atoms) with temperatures that are far greater than the average gas temperature due to the Frank-Condon effect. Thus emitting atoms produced by dissociative excitation are at much higher temperatures than the surrounding gas species resulting in a significantly wider line profile for these atoms. As argon is an atomic gas there are no dissociative excitation channels available, so the argon line width should serve as a good indicator of gas temperature. Comparing the emission widths for the profiles in figure 5 the 777nm nm line has a width that is approximately twice that of either the Ar 750 nm or O 844 nm lines. This indicates that a significant contribution is made to the 777 nm emission by dissociative excitation of O_2 molecule in the plasma, while dissociative excitation makes little contribution to emission at 844 nm. The width of the O^* (844) and Ar^*(750) lines recorded is determined by the instrument bandpass rather than the Doppler line widths which are too narrow to be measured with the spectrometer used. Previous authors working in regimes with low [O] content such as the O_2/Ar mixture examined in these experiments found that while dissociative excitation only makes a small overall contribution to the [O] density, it can contribute significantly to O emission, particularly at 777 nm [17].

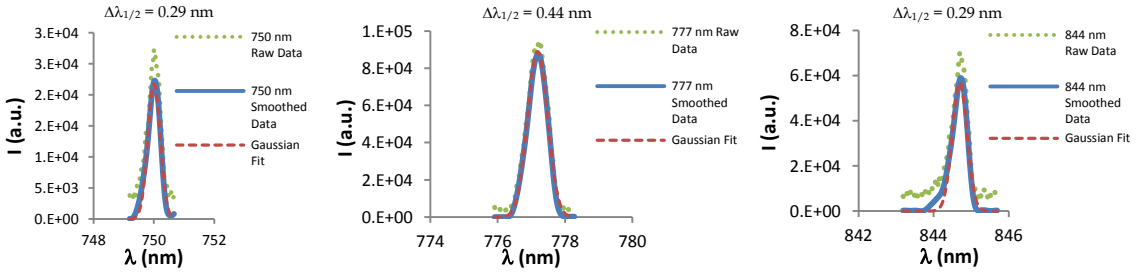

Figure 5: Emission line profiles for the 750 nm, 777 nm and 844 nm lines recorded during these experiments at 50W. The raw data was first smoothed and then an optimised Gaussian Fit was obtained using Excel Solver.

For plasmas with higher dissociation fractions such as fluorinated oxygen plasmas the dissociative contribution to oxygen emission is less important and the emission at 777nm and 844 nm should better represent [O] in the plasma. For this reason the line profiles of the 844 nm emission line were chosen for analysis and determination of [O] content in the plasma. Rate constants were calculated for electron excitation of the Ar^* 750 nm excited state ($k_e^{Ar(750)}$), O^* 844 state ($k_e^{O(844)}$) and the $O_2{}^*$ 844 nm dissociative excitation state ($k_{de}^{O(844)}$) using the PIC EEDF and cross section data available in the literature [30, 31, 16].
The results of the experiments are shown in figure 6 below. The pressure was kept constant at 100 mTorr and the RF power was ramped up from 50 W to 300 W in 50 W steps and emission spectra were recorded over the 700 nm – 900 nm range. The emission lines at 844 nm and 750 nm are used to calculate [O] using the actinometry technique. TALIF measurements were also recorded at each of the plasma settings by scanning the dye laser output wavelength across the appropriate wavelength range and recording the corresponding fluorescence emitted from the plasma. Absolute [O] values were obtained by calibrating the TALIF system using Xe gas fluorescence as discussed earlier. The TALIF data shows that the atomic oxygen density drops slightly with increasing RF power for constant pressure. This trend is somewhat unusual but one possible explanation is that the gas temperature increases with applied power as has been shown by Kielbauch *et al* [32]. This would lead to a reduced O_2 number density in the plasma as the number density is given by n = P/kT so increasing T will result in a reduced number density even though the pressure remains the same. Also, at higher temperatures

the rate of diffusion of O atoms to the walls will increase so enhanced atomic oxygen surface recombination will reduce the [O] value in the plasma.

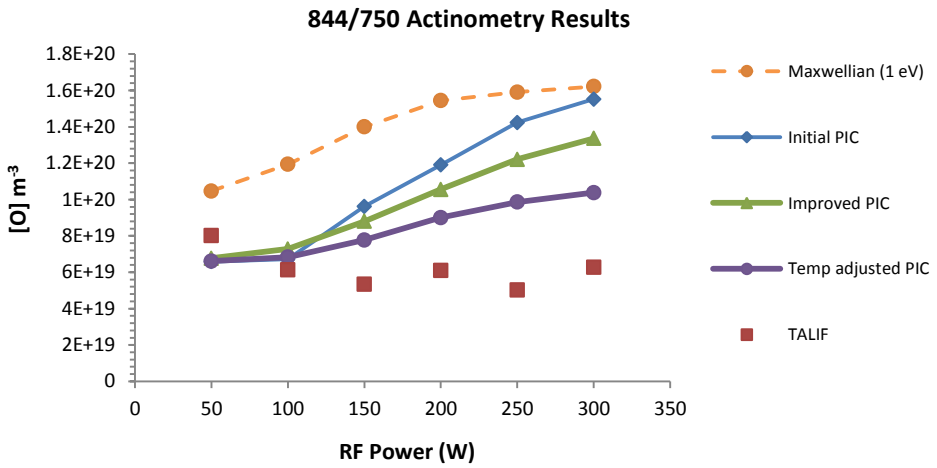

Figure 6: Plots of actinometry and TALIF results for [O] vs RF power at a pressure of 100 mTorr. Actinometry results using various PIC inputs are included to show the effect changing the PIC inputs have on the [O] values. Gas temperature variations were also included in the analysis.

Referring to figure 6, the magnitude of the actinometry and TALIF results obtained for [O] are in reasonable agreement though there is a slight discrepancy in the trend with the actinometry results showing an increase in [O] with RF power. To show the influence of the EEDF on the actinometry results, various EEDFS are used to generate rate constants for use in the actinometry model. As an initial approach to the problem, a Maxwellian EEDF for an electron temperature of 1eV is used to produce rate constants. The results are included in figure 6. This approach yielded the least satisfactory agreement between the TALIF and actinometry [O] values indicating this is not a particularly good choice of EEDF. The results obtained using PIC generated EEDFs give a marked improvement in actinometry results for [O], indicating that the EEDF generated in the simulation is a more realistic representation of the true form of the EEDF in the plasma. Three set of results using a PIC approach are included in the figure. The actinometry results obtained using the EEDF from the initial PIC simulation which give the poorest agreement for n_e (see figure 4) also gives the worst agreement with the TALIF results. However, the [O] values are still in better agreement with TALIF than the results obtained using a Maxwellian distribution. Using the rate constants obtained from the improved PIC simulation where the PIC n_e and experimental n_e match, the [O] results for actinometry and TALIF techniques show improved agreement. The method seems to work well at lower RF powers. However at higher powers the actinometry and TALIF results start to diverge. Incorporation of the temperature variations into the analysis brings the results into even better agreement reducing the difference in the actinometry and TALIS [O] results observed at higher RF powers.
This indicates that using the n_e value from the PIC code serves as a good metric for the reliability of the simulation and so to the reliability of the rate constants obtained. Furthermore for low dissociation fraction plasma such as that investigated in this work care must be taken to include other variables such as temperature effects to help improve the overall accuracy. In this work effect due to self-absorption are neglected, though recent work by Gudimenko *et al* indicate that this may have an effect under certain plasma operating conditions [33]. Also there is some concern that the viewports may be affected by the plasma due to deposition of material on the viewport or due to etching of the viewport particularly for fluorine containing plasmas. Further work is planned to investigate these effects.

4. Conclusion

A method has been proposed to attempt improve rate constants values for use in quantitative actinometry of [O] in a capacitively coupled plasma (CCP) system. PIC simulations were used to generate EEDFs which were then used to calculate the various rate constants required for use in the actinometry model. To optimise the simulations, electron density results from the simulation were

compared to experimental values obtained using a hairpin probe. The input parameters for the PIC were adjusted so the PIC electron densities matched the experimental ones. Using the corresponding EEDFs the $k_e^{Ar(750)}$, $k_e^{O(844)}$ and $k_{de}^{O(844)}$ rate constants were calculated for each of the plasma conditions allowing [O] to be determined using the I^{844}/I^{750} line ratio recorded for each plasma conditions. Comparing the actinometry [O] values to TALIF values recorded under the same plasma conditions the best agreement between the actinometry and TALIF data was achieved by optimising the PIC simulation using the method proposed in this work. Further improvement in the [O] agreement was obtained by including gas temperature changes resulting for the different plasma conditions examined.

Acknowledgements: This material is based upon work supported by the Science Foundation Ireland under Grant no. 08/SRC/I1411. Also, I would like to thank Dr Aidan Cowley for his helpful input on the PIC simulations, and Mr. Conor Murphy for his technical assistance with the plasma system.

References

[1] Brown M S, Scofield J D and Ganguly B N, J Appl. Phys. 94 (2003) 822.
[2] Selamoglu N, Murcha J A, Ibbitson D E and Flamm D L, J. Vac. Sci. Technol. B 7 (1989) 1345.
[3] Egitto F D, Pure and Appl. Chem. 62 (1990) 1699.
[4] Burns G P, Baldwin I S, Hastings M P and Wilkes J G, J. Appl. Phys. 66 (1989) 2320.
[5] D'Agostino r, Cramarossa F, De Benedictus S and Ferraro G, J. Appl. Phys. 52 (1981) 1259.
[6] Stoffels E, Keift I E, Sladek R E J, van den Bedem L J M, van der Laan E P and Steinbuch M, Plasma Sources Sci. Technol. 15 (2006) S169.
[7] Hopkins M B, J. Res. Natl. Inst. Stand. Technol. 100 (1995) 415.
[8] I Sorli, R Rocak, J. Vac. Sci. Technol. A 18 (2000) 338.
[9] Babič D, Poberaj I and Mozetič M, Rev. Sci. Instrum. 72 (2001) 4110.
[10] Brake M, Hinkle J, Asmussen J, Hawley M and Kerber R, Plasma. Chem. Plasma Process. 3 (1983) 63.
[11] H. F. Döbele, T Mosbach, K Neimi, V Schultz-von der Gathen, Plasma Sources Sci. Technol. 14 (2005) S31-S41.
[12] W R Harshbarger, R A Porter, T A miller and P Norton Appl. Spectrosc. 31 (1977) 201.
[13] J W Coburn and M Chen, J. Appl. Phys. 51 (1980) 3134.
[14] Walkup R E, Saenger K L and Selwyn G S, J. Chem. Phys 84 (1986) 2668.
[15] Collart E J H, Baggerman J A G and Visser R J, J. Appl. Phys. 78 (1995) 47.
[16] H M Katsch, A Tewes, E Quandt, A Goehlich, T Kawetzki, H. F Dobele, J. Appl. Phys. 88 (2000) 6232.
[17] Booth J P, Joubert O and Pelletier J, J. Appl. Phys. 69 (1991) 618.
[18] Pagnon D, Amorim J, Nahorny J, Touzeau M and Vialle M, J. Phys. D: Appl. Phys. 28 (1995) 1856.
[19] Granier A, Chéreau D, Henda K, Safafi R and Leprince P, J. Appl. Phys. 75 (1994) 104.
[20] Ershov A and Borysow J, Plasma Sources Sci. Technol. 16 (2007) 798.
[21] Bousquet A, Cartry G and Granier A, Plasma Sources Sci. Technol. 16 (2007) 597.
[22] Taylor K J, Tynan G R, J. Vac. Sci. technol. A. 23 (2005) 643.
[23] Neimi K, Reuter S, Graham L M, Waskoenig J, Knake N, Schulz-von der Gathen V and Gans T, J. Phys. D: Appl. Phys. 43 (2010) 124006.
[24] N S Braithwaite, Pure and Appl. Chem. 62 (1990) 1721.
[25] J S Jeng, J Ding, J W Taylor, N Hershkowitz, Plasma Sources Sci. Technol. 3 (1994) 154.
[26] M Aflori, J L Sullivan, Romanian Reports on physics 57 (2005) 71.
[27] Karkari S K, Gaman C, Ellingboe A R, Swindells I and Bradley J W 2007 Meas. Sci. Technol. 18 2649.
[28] Y Yamauchi and R Shimizu, Jap. J. Appl. Phys. 22 (1983) L227.
[29] P C smith, B Hu and N D Ruzic, J. Vac. Sci. Tech. A. 5 (1994) 2692.
[30] J E Chilton, J B Boffard, R S Schappe and C C Lin, Phy. Rev. A, 57, (1998), 267.
[31] R. R. Laher and F. R. Gilmore, J. Phys. Chem. Ref. Data 19, (1990), 277.

[32] M W Kielbauch, D B graves, J. Vac. Technol. A 32 (2003) 660.
[33] E Gudimenko, V Milosaljevic and S Daniels, Opt. Express 20 (2012) 12699.